Reusable Floating-Electrode Sensor for the Quantitative Electrophysiological Monitoring of a Nonadherent Cell

Van-Thao Ta,[†,‡] Juhun Park,[†] Eun Jin Park,[†] and Seunghun Hong[†,§,*]

[†]Department of Physics and Astronomy, and Institute of Applied Physics, Seoul National University, Seoul 151-747, Korea, [‡]Department of Chemistry, Hanoi National University of Education, Hanoi, Vietnam, and [§]Department of Biophysics and Chemical Biology, Seoul National University, Seoul, 151-747, Korea

ABSTRACT

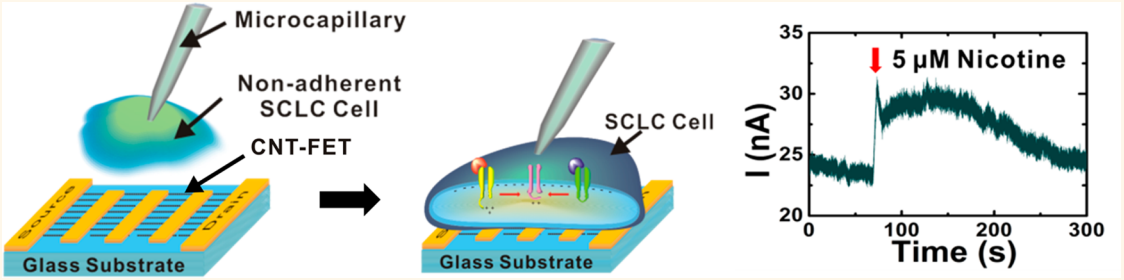

We report a *reusable* floating-electrode sensor based on aligned semiconducting single-walled carbon nanotubes for the *quantitative* monitoring of the electrophysiological responses from a *nonadherent* cell. This method allowed us to monitor and distinguish the real-time responses from *normal* and *small-cell lung cancer* (SCLC) cells to the addition of nicotine. The difference was attributed to the overexpressed nicotinic acetylcholine receptors (nAChRs) in the SCLC cells. The sensor was also utilized to monitor the effect of various drugs on the cells. The treatment with inhibitors such as genistin or daidzein was found to reduce Ca^{2+} influx in SCLC cells. Moreover, tamoxifen, though known as the antiestrogen compound, was found to only partly block the binding of daidzein to nAChRs. Significantly, the activities of *multiple* individual cells could be measured repeatedly using a *single* sensor device, enabling statistically meaningful measurements without errors from the device-to-device variations of the sensor characteristics. This capability of the *quantitative* monitoring of *nonadherent* cells should be a major breakthrough for electrophysiology research and various biomedical applications such as drug screening and therapeutic monitoring.

KEYWORDS: small-cell lung cancer cell · nicotinic acetylcholine receptors · carbon nanotube · nonadherent cell · field effect transistor

Nicotinic acetylcholine receptors (nAChRs) were found to be important regulators that modulate the release of growth angiogenic and neurogenic factors and stimulate cancer development and progression.[1−4] However, the current knowledge about nAChRs is almost exclusively based on the studies about *adherent* cells such as brain cells.[1] Recently, nAChRs were also found to be expressed with a high level on *nonadherent* cells such as small-cell lung cancer (SCLC) cells.[1,5,6] In order to understand the regulation via nAChRs in *nonadherent* cells, sensitive and versatile measurement techniques are required. Electrophysiological techniques have shown distinct advantages for the detection of bioelectrical signals resulting from the orchestrated activities of ion channels embedded within cell membranes like those of nAChRs.[7−10] For example, in a patch clamp method, one can place a probe on a specific cell and monitor ion channel activity with both high signal-to-noise ratio and high temporal resolution.[11,12] However, a patch clamp method needs rather complicated cell manipulation steps and, thus, usually requires a skilled operator. On the other hand, microscale field effect transistors (FETs) or electrode sensors have been utilized to easily measure the activities of *adherent* cells grown on the devices without complicated manipulation steps.[13−16] Recently, nanoscale devices have been studied as a tool to monitor the electrical activities of various cells with a high resolution.[17−20]

* Address correspondence to seunghun@snu.ac.kr.

Received for review October 11, 2013 and accepted February 3, 2014.

Published online February 03, 2014
10.1021/nn4053155

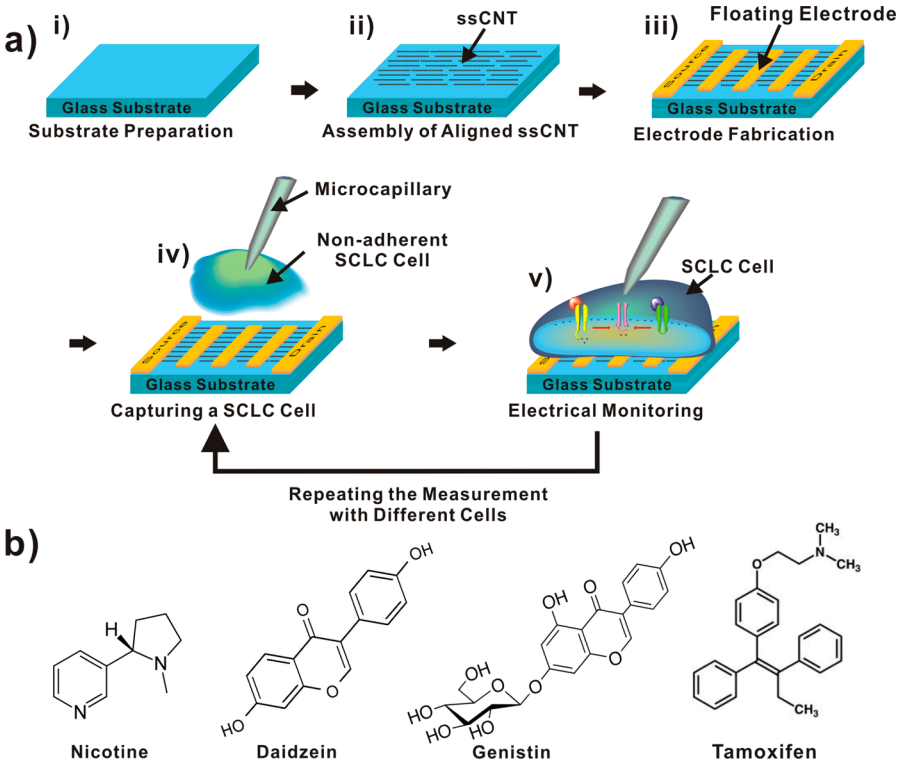

Figure 1. Schematic diagram depicting the experimental procedure and molecular formula of the chemicals used in the experiment. (a) Schematic diagram showing the experimental procedure: (i) preparation of clean glass substrates; (ii) assembly of aligned ssCNT networks on the glass substrate *via* the spin-coating method; (iii) fabrication of electrodes *via* conventional microfabrication processes; (iv) capturing a nonadherent SCLC cell floating in a solution; (v) placing the cell on the sensor surface and measuring its electrophysiological activity using the sensor. Steps (iv) and (v) can be repeated for a different cell using the same sensor device. (b) Chemical structures of nicotine, daidzein, genistin, and tamoxifen.

However, the characteristics of such nanoscale devices may vary significantly from one device to another, and each device can measure only cells grown on it. Thus, it is often very difficult to compare the measurement results using different devices or to obtain statistically meaningful quantitative measurement results. Furthermore, most of the previous methods based on solid-state devices such as electrode or FET devices could be used to monitor the electrical activities of only *adherent* cells fixed on the device surface.

Herein, we report a *reusable* floating-electrode sensor (FES) based on aligned semiconducting single-walled carbon nanotubes (ssCNTs) for the *quantitative* monitoring of the electrophysiological responses from a *nonadherent* cell. In this method, we first fabricated a FES device that was composed of *aligned* ssCNT network-based channels separated by multiple *floating electrodes*. Then, a single SCLC cell in solution was captured using a microcapillary and placed on the sensor to monitor the electrophysiological response of the SCLC cell to various chemical stimuli. Significantly, the cell immediately made a good contact with the floating electrode structures in the FES device, allowing us to monitor the electrophysiological responses from the cell. Note that in this process, after a measurement, we could pick up another cell and repeat the measurement using the same device, which allowed us to obtain reliable results without errors from the variation of sensor device characteristics. Using this method, we could measure the electrophysiological response of a single floating SCLC cell as well as a normal lung cell to the addition of nicotine. The rather large electrophysiological response of the SCLC cell to nicotine was attributed to the overexpressed nAChRs in the SCLC cell.[5] Significantly, we utilized only a *single* FES device to measure the effect of various regulating drugs such as genistin, daidzein, and tamoxifen on the nAChR activity of *multiple* SCLC cells, which enabled a statistically meaningful quantitative analysis without errors from device-to-device variations. The results indicate that the treatment of inhibitors such as genistin and daidzein can dramatically reduce Ca^{2+} influx in SCLC cells as expected.[21] Furthermore, tamoxifen, which has been known as the antagonist, was found to only partly block the binding of daidzein to nAChRs. This quantitative monitoring capability for the electrical activity of nonadherent cells can be a major breakthrough in electrophysiology research and should open up various biomedical applications such as drug screening and therapeutic monitoring.

RESULTS AND DISCUSSION

Figure 1a illustrates the fabrication procedures of a FES based on aligned ssCNTs. The method we used for

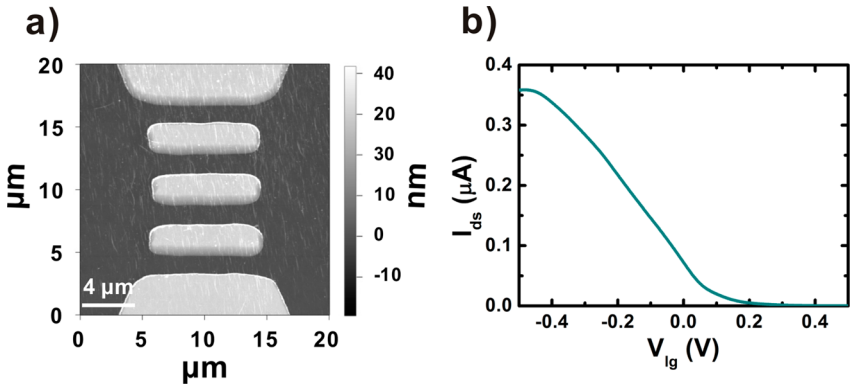

Figure 2. Characterization of a floating-electrode sensor based on aligned ssCNT networks. (a) AFM topography image of a FES device that has three floating electrodes. Individual floating electrodes have dimensions of 12 μm width and 2 μm length. (b) Liquid gating effect of a FES device. Here, a Ag/AgCl electrode was used as a liquid gate, and the gate bias was swept from −0.5 to 0.5 V with the source−drain bias of 0.1 V.

the fabrication of FES devices was similar to that reported previously.[22] In brief, a clean glass substrate was prepared by eliminating hydrocarbon materials from the glass surface via a piranha cleaning process (Figure 1a-i). The networks of aligned ssCNT were assembled on the glass substrate by the spin-coating method (Figure 1a-ii). Then, metal electrodes were formed by photolithography techniques and the thermal deposition of Pd and Au (30 nm Au on 10 nm Pd) followed by a lift-off process (Figure 1a-iii). The sensor was then placed in the solution of SCLC cells, and a specific SCLC cell of interest floating in the solution was captured using a microcapillary (Figure 1a-iv). The captured cell was placed on the FES surface, and the electrophysiological measurement was performed using the sensor (Figure 1a-v). In the case of normal cells, which were adherent to solid substrates, the cells were directly grown on the sensor surfaces and utilized for the measurement. Here, the cell made direct contact with the floating electrodes of the FES device, and the change in potential on the extracellular side of the cell membrane altered the conductance of the device.[22] Note that the measurement steps were rather simpler than the patch clamp method. In the patch clamp method, a microcapillary is moved on a cell membrane, and suction is applied to form a hole on the cell membrane. In these processes, a high-resistance seal should be maintained to obtain a clear signal, which is often very difficult and requires a highly skilled operation. However, in our method, one can pick up general nonadherent cells floating in a solution and hold the cell on the active area of a FES device to monitor its electrical activity. We do not need to make a hole on the cell membrane or maintain a high-resistance seal using the microcapillary, which enables simple and nondestructive measurements. Significantly, one can repeat the measurement for different cells with the same device, enabling statistically meaningful quantitative measurements. Since this simple method can be applied for the reliable quantitative electrophysiological monitoring of general cells including nonadherent cells, it can be a powerful tool for biomedical research and applications.

Figure 2a shows the AFM topography image of the channel region in a FES device. Each floating electrode had the dimensions of 12 μm width and 2 μm length. Note that the ssCNTs in the device were well-aligned between the electrodes. Previous works show that the alignment of CNTs could reduce the formation of metallic paths by removing lateral connections, and it improved the transconductance of the device channels and the sensor performance.[23,24] In our devices, although we utilized purified semiconducting CNTs, the alignment of CNTs is expected to further reduce the possible metallic paths and improve the performance of our sensor devices. Furthermore, it was also reported that the addition of floating electrode structures increased the number of modulating Schottky barriers, resulting in the enhanced sensitivity of biological sensors.[22]

The electrical properties of a FES device were also investigated. Figure 2b shows the gating effect curve obtained by using a liquid gate. Here, we utilized a Ag/AgCl electrode as a liquid gate to sweep a gate bias voltage (V_{lg}) from −0.5 to 0.5 V, while maintaining the source−drain bias of 0.1 V. It shows a decreasing current with an increasing positive gate bias, indicating the typical p-type characteristics of CNT devices. Significantly, the source−drain current decreased very quickly and could be turned off even at a small positive gate bias voltage, indicating ideal characteristics for sensor applications. Presumably, the enrichment of semiconducting CNTs as well as the alignment strategy drastically reduced the formation of metallic paths and, thus, improved their transconductance.[23,24]

Figure 3a depicts the mechanism of Ca^{2+} influx stimulated by nicotine *via* nAChR activation. SCLC cells are known to have overexpressed nAChRs such as α7 nAChRs and α4 nAChRs on their membrane.[1,5] In the resting state, the gates on the intracellular side of two

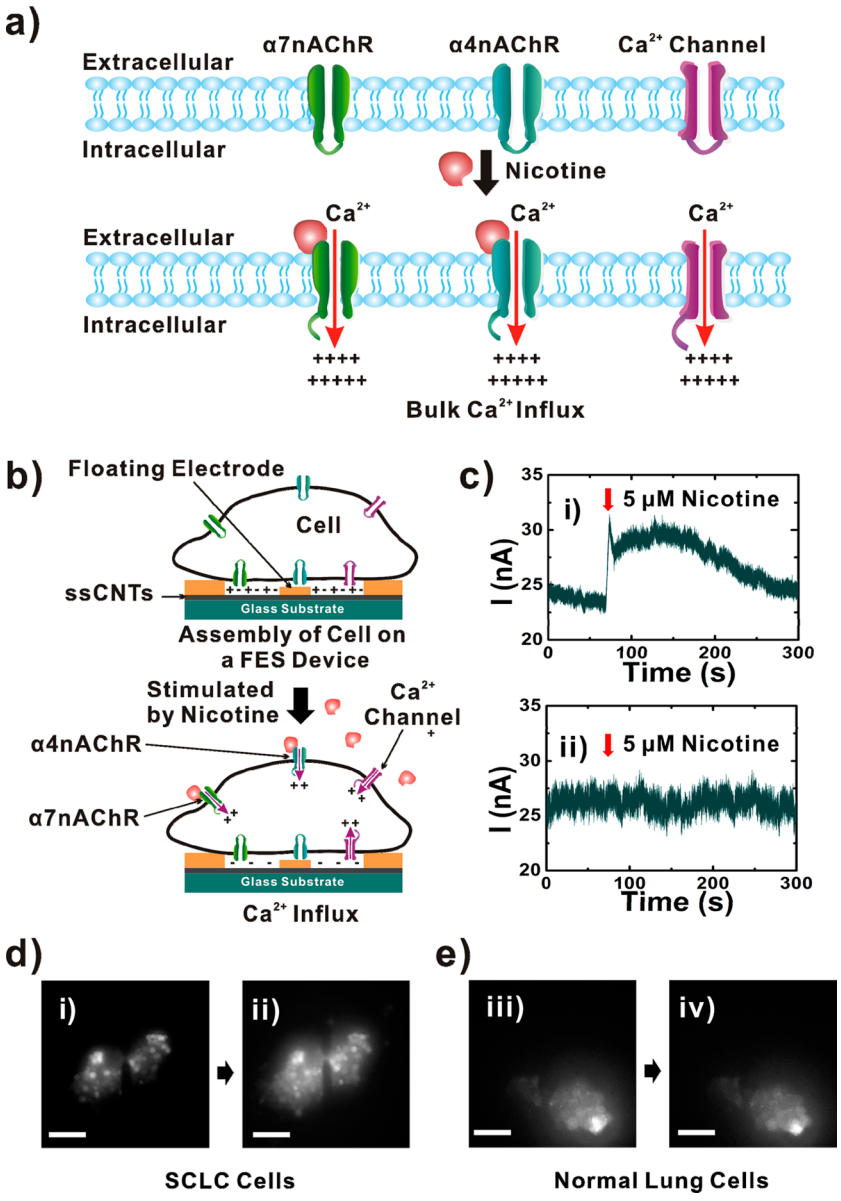

Figure 3. Electrophysiological response of a SCLC cell and a normal lung cell to the addition of nicotine. (a) Schematic drawing depicting the mechanism of Ca^{2+} influx stimulated by a nicotinic ligand via nAChRs activation. (b) Schematic diagram showing the sensing mechanism of our FES device for the monitoring of Ca^{2+} influx stimulated by nAChRs in a cell. (c) Real-time conductance data measured by FES devices with (i) an SCLC cell and (ii) a normal lung cell during the addition of 5 μM nicotine. The FES device exhibited conductance changes only with the SCLC cells. The result clearly indicates that our floating-electrode sensor could distinguish individual cells *with* or *without* nAChRs. (d) Fluorescent images of the SCLC cell obtained before (i) and after (ii) the addition of 5 μM nicotine. (e) Fluorescent images of the normal lung cell obtained before (i) and after (ii) the addition of 5 μM nicotine. The scale bar represents 100 μm.

ligand-gated nAChRs and the gates of voltage-activated Ca^{2+} channels are closed. When nicotine binds to the nAChRs, the conformation of the receptor subunits is changed, resulting in the opening of the receptor gates. Thus, Ca^{2+} flows into the cell through the opened channels of nAChRs. This initiates depolarization of the cell (Figure 3b). In turn, this change in electric charges opens the gates of the voltage-gated Ca^{2+} channel, resulting in the further depolarization of the cell and the increase of the negative potential on the extracellular side of the plasma membrane. Note that our FES devices exhibited increased currents by a negative gate bias (Figure 2b). Thus, when the device is in contact with the extracellular side of the cells, the increased negative potential on the extracellular side of the plasma membrane caused by nicotine should result in the increased electrical currents in the FES device.[13,25]

Figure 3c shows the real-time conductance measurement results obtained by utilizing FES devices with either an SCLC cell or a normal lung cell during the addition of nicotine. When 5 μM nicotine was added, a FES device with the SCLC cell exhibited the large current change of 6.2 nA (Figure 3c-i), whereas, when

5 μM nicotine was added to the normal lung cell, there were no significant changes in electric currents (Figure 3c-ii). Also, the addition of 5 μM nicotine did not affect the current of a FES device without any cell and that with a normal lung cell that was not adhered on the device (Figures S1 and S2 in the Supporting Information). The sharp increase of the electric current in the case of the SCLC cell can be explained by the interactions of nicotine with nAChRs overexpressed only in the SCLC cell. The binding of nicotine to nAChRs induced the influx of Ca^{2+} into the cell, resulting in a relatively negative potential in the vicinity of our FES device. Since our FES devices exhibited *p-type* characteristics, the decrease of potential should have resulted in the increase of its electrical currents.[26] To confirm the repeatability of the sensing experiments, we repeated the measurements for SCLC cells using a FES device three times and found the changes in electric currents were similar to each other (Figure S3 in the Supporting Information). This result clearly shows that our FES devices could selectively measure the activity of nAChRs and identify the overexpression of nAChRs only in SCLC cells. Since our method measures the potential change of plasma membranes even for *nonadherent* cells, we can expect that our method can be utilized for the study of general electrically excitable cells (both adherent and nonadherent) such as neurons, myocytes, or endocrine cells.

Since our method was compatible with conventional fluorescence methods, we could perform the fluorescence Ca^{2+} assays for the confirmation of Ca^{2+} influx on the cells assembled on our FES devices. Figure 3d and e shows the responses of SCLC cells and normal lung cells assembled on a FES by the addition of nicotine, respectively. In this experiment, cell lines were first incubated in a Ca^{2+}-free Krebs-Ringer-Hepes (KRH) solution including 2 μM fluo-4-AM as a Ca^{2+} indicator so that the Ca^{2+} indicator diffused into and was trapped inside the cells. Note that the fluorescent intensity in SCLC cells increased significantly when 5 μM nicotine was added. The time course of the fluorescence intensity is shown in Figure S4a in the Supporting Information. The time course showed a similar behavior to the real-time conductance measurement data in Figure 3c-i. However, there was no significant change in the fluorescent intensity of normal lung cells (Figure S4b in the Supporting Information). It confirms that nAChRs were overexpressed only on the SCLC cells, and they were working properly even on our FES devices.[1,27] This result was also consistent with that from electrophysiological measurement as shown in Figure 3c, where Ca^{2+} influx was found only in SCLC cells.

Figure 4a depicts the mechanism of Ca^{2+} influx on a SCLC cell modulated by phytoestrogens such as genistin and daidzein. Phytoestrogens are known as inhibitors that have a high affinity with α4 nAChRs and inhibit the receptors from interacting with nicotine.[28] Thus, when nicotine is added, Ca^{2+} influx through α4 nAChRs is blocked and we should observe a reduced overall Ca^{2+} influx into the SCLC cell.[1,21] In turn, this decrease of membrane depolarization could also reduce the gate-opening of voltage-gated Ca^{2+} channels and additional influx of Ca^{2+}. In the case of a partial blocking, the *quantitative* monitoring of electrophysiological responses can enable the quantitative analysis of the effect of drugs. However, in most of the previous works, one had to use different devices to measure the effect from multiple cells, and the variation of device characteristics often hindered reliable statistical analysis. For example, although the sensor signals from different CNT-based sensors can be calibrated by normalizing the sensor signals, the normalized results still exhibited some distribution due to structural variations in CNT network channels such as CNT network connectivity.[29] In our method, after a measurement on one cell, we can pick other cells and repeat the measurement with the same device. Thus, our method can produce reliable quantitative measurement results without errors from the variation of device characteristics, which can be a significant advantage for the quantitative analysis of drug effects.

Figure 4b shows the real-time electrophysiological responses of individual SCLC cells to 5 μM nicotine when it was pretreated with different phytoestrogens. Note that all these data were measured using a *single* FES device, which enabled the quantitative comparison of the drug effects without errors from device-to-device variations. In the measurement, an SCLC cell assembled on the FES device was bathed in 300 μL of Ca^{2+}-free KRH solution including 100 μM genistin (Figure 4b-i), 100 μM daidzein (Figure 4b-ii), or 100 μM tamoxifen as well as 100 μM daidzein (Figure 4b-iii) for 10 min. A Ag/AgCl electrode with a bias of -0.1 V was utilized as a liquid gate electrode. To trigger the nAChRs of the SCLC cell, 300 μL of KRH solution consisting of 10 μM nicotine was added so that the final concentration of nicotine reached 5 μM. The concentration of nicotine was fixed to 5 μM to compare the effect of phytoestrogens with different concentrations. Note that the current change of the FES device with the SCLC cell treated with genestin (Figure 4b-i) was $\sim$4.8 nA, which was much smaller than that of the device with an untreated SCLC cell ($\sim$6.2 nA in Figure 3b-i), indicating that the genestin worked as an inhibitor. Interestingly, the SCLC cell treated with daidzein (Figure 4b-ii) exhibited a current change of 2.9 nA, which was even smaller than that for the SCLC cell treated with genestin. This indicates that the daidzein is a more efficient inhibitor than genestin, which is consistent with previous works using adherent cells.[21] However, when an SCLC was treated with both daidzein and tamoxifen, the electrophysiological response (Figure 4b-iii) showed the effect of tamoxifen, an antiestrogen, on the Ca^{2+} influx regulation of daidzein. The SCLC cell treated with both tamoxifen and daidzein

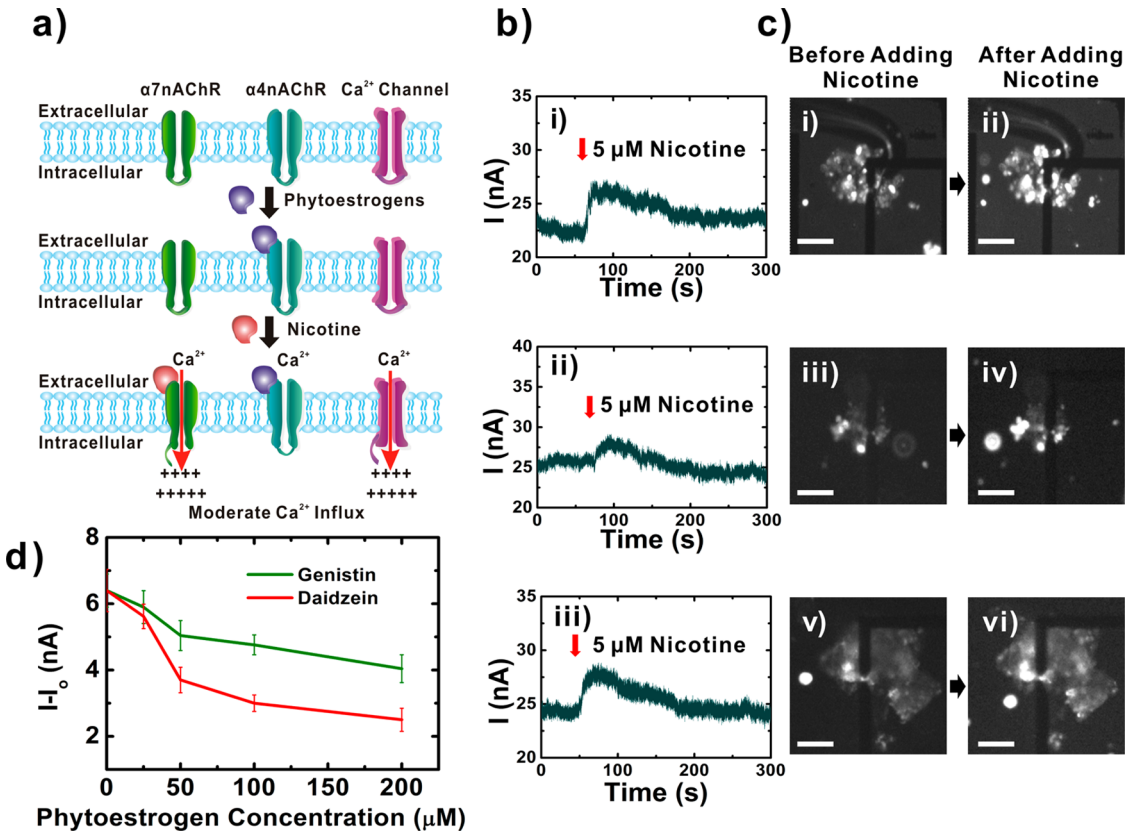

Figure 4. Quantitative electrophysiological monitoring of a SCLC cell regulated by phytoestrogens. All electrophysiological measurements were performed using the same FES device. (a) Schematic diagram depicting the effect of phytoestrogen on the Ca^{2+} influx into an SCLC cell. (b) Real-time electrophysiological response of SCLC cells to the addition of 5 μM nicotine when the cell was pretreated with (i) 100 μM genistin, (ii) 10 μM daidzein, or (iii) 100 μM tamoxifen and 100 μM daidzein. (c) Fluorescent Ca^{2+} assay images of SCLC cells obtained before (*left*) and after (*right*) the addition of 5 μM nicotine. The cells were pretreated with (i, ii) genistin; (iii, iv) daidzein; and (v, vi) tamoxifen and daidzein. (d) Modulation of Ca^{2+} influx of SCLC cells by varying phytoestrogen concentration. The SCLC cells were pretreated with various concentrations of genistin or daidzein in the range 25−200 μM, and their responses to 5 μM nicotine were monitored using a single FES device. The scale bar represents 100 μm.

exhibited a current change of ~4.5 nA. Although it was larger than that of the SCLC cell treated with only daidzein (~2.9 nA), it was still much smaller than that of the untreated cell (~6.2 nA in Figure 3c), indicating that tamoxifen did not completely block the effect of daidzein. This result implies that the inhibition of daidzein was not mediated through classical estrogen receptors or similar binding sites as reported in previous works on adherent brain cells.[1] These results clearly show that the binding mechanism of phytoestrogens with nAChRs could be studied quantitatively utilizing our FES device.

The *left* and *right* images in Figure 4c show fluorescent Ca^{2+} assay images of SCLC cells *before* and *after* being stimulated by nicotine, respectively. Here, SCLC cells were first incubated with fluo-4-AM, a Ca^{2+} indicator, so that the cells included the Ca^{2+} indicator. Then, SCLC cells were pretreated with 100 μM genistin (Figure 4c-i), 100 μM daidzein (Figure 4c-ii), or 100 μM tamoxifen + 100 μM daidzein (Figure 4c-iii) for 10 min, and then the cells were stimulated by 5 μM nicotine. Note that the fluorescence intensity increased even though the cells were treated with inhibitors, which is consistent with the measurement results from our FES devices shown in Figure 4b. However, it should be noted that since the shape of SCLC cells varies significantly, it was very difficult to perform a *quantitative* analysis on the drug effect.

Figure 4d shows the dependence of the Ca^{2+} influx regulation of SCLC cells on various phytoestrogen concentrations. Here, SCLC cells were first treated with genistin or daidzein with various concentrations of 25−200 μM. Then, the electrophysiological response of the SCLC cells to 5 μM nicotine was monitored using a FES device. For a reliable statistical analysis, we repeated the measurement for multiple SCLC cells and performed three measurements for each phytoestrogen concentration using the same FES device (Figure S5 in the Supporting Information). Note that, even after 27 measurements, the current level of the FES device remained similar to the original current level, which indicates our FES devices can be used for repeated sensing measurements (Figure S6 in the Supporting Information). The results show that Ca^{2+} influx was reduced with an increased concentration of

inhibitors, genistin or daidzein. Moreover, daidzein exhibited a better inhibition than genistin, which is consistent with previous works on different cells.[21] However, until now, such a quantitative study of drug effects could be done mostly on adherent cells such as brain cells. Thus, the capability of quantitative real-time monitoring of electrical activities in *small nonadherent* cells can be a major breakthrough in electrophysiological research and should open up many significant applications.

CONCLUSIONS

We demonstrated a simple but versatile method based on a reusable floating-electrode sensor for quantitative monitoring of the electrophysiological response of a single nonadherent cell. In this method, we could easily select a specific SCLC cell floating in solution and directly measure its extracellular transmembrane potential in real time. We could clearly observe the different responses from the *normal* and *SCLC* cells to nicotine, which was attributed to overexpressed nAChR in the SCLC cells. Furthermore, the electrophysiological response of multiple SCLC cells could be measured using the same FES device without errors from the device-to-device deviation of device characteristics, which allowed us to perform a reliable statistical analysis of the effect of various regulating drugs on the nAChR activity. The results revealed that treatment with inhibitors such as genistin and daidzein can dramatically reduce Ca^{2+} influx in SCLC cells. In addition, although known as an antagonist, tamoxifen only partly blocked the binding of daidzein to nAChRs. Since our measurement method allows us to monitor the electrical activities of any desired cell (both *adherent* and *nonadherent*) at a single-cell level with a rather simple step, it promises various biomedical applications such as drug screening and therapy monitoring.

MATERIALS AND METHODS

Materials. Purified semiconducting single-walled carbon nanotubes were purchased from NanoIntegris Inc. (USA) and used as received. The ssCNTs have a diameter of 0.7−2 nm and a length of 2−3 μm. Nicotine, genistin, daidzein, tamoxifen, and other chemical reagents were purchased from Sigma-Aldrich (USA) and used as received.

Fabrication of the Floating-Electrode Sensor Based on Aligned Semiconducting Single-Walled Carbon Nanotubes. First, glass substrates were immersed in piranha solution (H_2SO_4/H_2O_2 = 3:1) to eliminate hydrocarbon materials on the surface. Purified semiconducting single-walled CNTs in a powder form were sonicated for 30 min in *o*-dichlorobenzene (0.005 mg/mL) for the dispersion of the CNTs. To assemble ssCNTs on the glass substrate in an aligned formation, ssCNTs in the suspensions were spin-coated on the SiO_2 substrates at 5000 rpm. The metal electrodes were formed by photolithography and thermal deposition of Pd and Au (30 nm Au on 10 nm Pd) followed by a lift-off process. Finally, we covered the source and drain electrodes with an aluminum oxide layer by the ALD to eliminate leakage currents from the electrodes into a buffer solution. To open specific regions of electrodes, a photolithography was performed. The FES device was immersed in H_3PO_4 solution (85% by weight in H_2O) at 90 °C for 3 min to etch aluminum oxide in the desired regions.

AFM Imaging Procedure. The AFM imaging of floating electrodes and ssCNTs on a glass substrate was performed by using a commercial AFM system (MFP-3D, Asylum Research) in an intermittent mode

Measurement Procedure for the Liquid Gating Effect of a FES Device. A Ag/AgCl electrode was utilized to apply a liquid gate bias (V_{lg}) through the PBS buffer solution onto a FES device. For the measurement, a gate bias was swept from −0.5 to 0.5 V while maintaining a source−drain bias of 0.1 V. The source−drain currents of the FES devices were measured by a semiconductor characterization system (Keithley, 4200, USA).

Cell Culture Procedure. Human SCLC cell lines (NCI-H146, nonadherent) and human normal lung cells (WI-38 VA-13, adherent) were purchased from the Korean Cell Line Bank (KCLB). NCI-H146 cells were grown in RPMI medium supplemented with fetal bovine serum (10% v/v), L-glutamine (2 mM), penicillin (100 U/mL), and streptomycin (100 μg/mL) at 37 °C in an atmosphere of 5% CO_2. WI-38 VA13 cells were grown in minimum essential medium (MEM), supplemented as above.

Electrophysiological Measurement of Ca^{2+} Influx in a Normal Lung Cell Using a FES Device. For the electrophysiological measurement of Ca^{2+} influx, a FES device was first sterilized and subsequently coated with fibronectin. Then, the FES device was placed in a live-cell imaging chamber. As an adherent normal lung cell, WI-38 VA-13 cells were grown on the surface of the FES device at 37 °C in an atmosphere of 5% CO_2 for 4 days to reach confluence. The grown normal lung cells were washed three times with Ca^{2+}-free KRH solution containing (in mM) 150 NaCl, 5 KCl, 1.2 $MgSO_4$, and 1.2 KH_2PO_4, 6 glucose, and 25 Hepes-NaOH (pH 7.4), and, then, they were incubated in the same solution with 2 μM fluo-4-AM for 30 min. The normal cells were again washed with a Ca^{2+}-free KRH solution three times; then 300 μL of Ca^{2+}-free KRH solution was added onto the channel regions of the FES device. For the electrophysiological measurement, a source−drain bias (V_{sd}) of 100 mV was applied on the FES device, and the source−drain currents were monitored by a data acquisition system (National Instruments, NI-9215(A)). For the detection of calcium influx, 300 μL of nicotine solution with a concentration of 10 μM in KRH (containing 4 μM Ca^{2+}) solution was introduced into the buffer solution.

During the measurement process, cells were also visualized simultaneously using a fluorescence microscope (Olympus, JP/IX71-21PH) equipped with an EMCCD (Andor, iXon3 897) and a mercury lamp (Nikon). Fluorescent measurements were performed with the *excitation* and *emission* at *495* nm and *516* nm, respectively.

Electrophysiological Measurement of Ca^{2+} Influx in an SCLC Cell Using a FES Device. NCI-H146 cells, which are nonadherent SCLC cells, were plated on a 24-well plate for 4 days at 37 °C in an atmosphere of 5% CO_2 and washed three times with Ca^{2+}-free KRH solution. Then, they were incubated in the same solution with 2 μM fluo-4-AM for 30 min and washed with a Ca^{2+}-free KRH solution three times. Then 300 μL suspensions of the SCLC cells were transferred to a FES device assembled in a live-cell imaging chamber. In the chamber, an SCLC cell was manually picked up and assembled on the FES channel region by using a micromanipulator. Usually, it took about 30 s for adjusting the position of a cell on a FES channel region. For the study of drug effects, phytoestrogens with various concentrations in the range 25 to 200 μM were added into the chamber and then incubated for 10 min. The FES device was connected with the data acquisition system. Both electrophysiological and fluorescent measurements were then performed in the same processes as described above for the normal lung cell.

Conflict of Interest: The authors declare no competing financial interest.

Acknowledgment. This work was supported by National Research Foundation grant (2009-0079103). SH acknowledges the support from the BioNano Health-Guard Research Center funded by the Ministry of Science, ICT & Future Planning of Korea as Global Frontier Project (H-GUARD_2013M3A6B2078961).

Supporting Information Available: This material is available free of charge *via* the Internet at http://pubs.acs.org.

REFERENCES AND NOTES

1. Schuller, H. M. Is Cancer Triggered by Altered Signalling of Nicotinic Acetylcholine Receptors? *Nat. Rev. Cancer* **2009**, *9*, 195–205.
2. Schuller, H. M. Cell Type Specific, Receptor-Mediated Modulation of Growth Kinetics in Human Lung Cancer Cell Lines by Nicotine and Tobacco-Related Nitrosamines. *Biochem. Pharmacol.* **1989**, *38*, 3439–3442.
3. Maneckjee, R.; Minna, J. D. Opioid and Nicotine Receptors Affect Growth Regulation of Human Lung Cancer Cell Lines. *Proc. Natl. Acad. Sci. U.S.A.* **1990**, *87*, 3294–3298.
4. Schuller, H. M.; Orloff, M. Tobacco-Specific Carcinogenic Nitrosamines. Ligands for Nicotinic Acetylcholine Receptors in Human Lung Cancer Cells. *Biochem. Pharmacol.* **1998**, *55*, 1377–1384.
5. Plummer, H. K.; Dhar, M.; Schuller, H. M. Expression of the α7 Nicotinic Acetylcholine Receptor in Human Lung Cells. *Respir. Res.* **2005**, *6*, 29.
6. Sartelet, H.; Maouche, K.; Totobenazara, J.; Petit, J.; Burlet, H.; Monteau, M.; Tournier, J. M.; Birembaut, P. Expression of Nicotinic Receptors in Normal and Tumoral Pulmonary Neuroendocrine Cells (PNEC). *Pathol. Res. Pract.* **2008**, *204*, 891–898.
7. Dunlop, J.; Bowlby, M.; Peri, R.; Vasilyev, D.; Arias, R. High-Throughput Electrophysiology: An Emerging Paradigm for Ion-Channel Screening and Physiology. *Nat. Rev. Drug Discovery* **2008**, *7*, 358–368.
8. Pui, T. S.; Sudibya, H. G.; Luan, X.; Zhang, Q.; Ye, F.; Huang, Y.; Chen, P. Non-Invasive Detection of Cellular Bioelectricity Based on Carbon Nanotube Devices for High-Throughput Drug Screening. *Adv. Mater.* **2010**, *22*, 3199–3203.
9. Osorio, N.; Delmas, P. Patch Clamp Recording from Enteric Neurons in Situ. *Nat. Protoc.* **2011**, *6*, 15–27.
10. Lipstein, N.; Sakaba, T.; Cooper, B. H.; Lin, K. H.; Strenzke, N.; Ashery, U.; Phee, J. S.; Taschenberger, H.; Neher, E.; Brose, N. Dynamic Control of Synaptic Vesicle Replenishment and Short-Term Plasticity by Ca^{2+}-Calmodulin-Munc13-1 Signaling. *Neuron* **2013**, *79*, 82–96.
11. Sakmann, B.; Neher, E. Patch Clamp Techniques for Studying Ionic Channels in Excitable Membranes. *Annu. Rev. Physiol.* **1984**, *46*, 455–472.
12. Molleman, A. *Patch Clamping: An Introductory Guide to Patch Clamp Electrophysiology*; Wiley: New York, 2003.
13. Peitz, I.; Voelker, M.; Fromherz, P. Recombinant Serotonin Receptor on a Transistor as a Prototype for Cell-Based Biosensors. *Angew. Chem., Int. Ed.* **2007**, *46*, 5787–5790.
14. Hutzler, M.; Lambacher, A.; Eversmann, B.; Jenkner, M.; Thewes, R.; Fromherz, P. High-Resolution Multitransistor Array Recording of Electrical Field Potentials in Cultured Brain Slices. *J. Neurophysiol.* **2006**, *96*, 1638–1645.
15. Hai, A.; Shappir, J.; Spira, E. M. In-Cell Recordings by Extracellular Microelectrodes. *Nat. Methods* **2010**, *7*, 200–202.
16. Sanchez-Vives, M. V.; McCormick, D. A. Cellular and Network Mechanisms of Rhythmic Recurrent Activity in Neocortex. *Nat. Neurosci.* **2000**, *3*, 1027–1034.
17. Duan, X.; Gao, R.; Xie, P.; Cohen-Karni, T.; Qing, Q.; Choe, H. S.; Tian, B.; Jiang, X.; Lieber, C. M. Intracellular Recordings of Action Potentials by an Extracellular Nanoscale Field-Effect Transistor. *Nat. Nanotechnol.* **2012**, *7*, 174–179.
18. Tzahi, C. K.; Casanova, D.; Cahoon, J. F.; Qing, Q.; Bell, D. C.; Lieber, C. M. Synthetically Encoded Ultrashort-Channel Nanowire Transistors for Fast, Pointlike Cellular Signal Detection. *Nano Lett.* **2012**, *12*, 2639–2644.
19. Patolsky, F.; Timko, B. P.; Yu, G.; Fang, Y.; Greytak, A. B.; Zheng, G.; Lieber, C. M. Detection, Stimulation, and Inhibition of Neuronal Signals with High-Density Nanowire Transistor Arrays. *Science* **2006**, *313*, 1100–1104.
20. Robinson, J. T.; Jorgolli, M.; Shalek, A. K.; Yoon, M. H.; Gertner, R. S.; Park, H. Vertical Nanowire Electrode Arrays as a Scalable Platform for Intracellular Interfacing to Neuronal Circuits. *Nat. Nanotechnol.* **2012**, *7*, 180–184.
21. Nakazawa, K.; Ohno, Y. Block by Phytoestrogens of Recombinant Human Neuronal Nicotinic Receptors. *J. Pharmacol. Sci.* **2013**, *93*, 118–121.
22. Kim, B.; Lee, J.; Namgung, S.; Kim, J.; Park, J. Y.; Lee, M. S.; Hong, S. DNA Sensors Based on CNT-FET with Floating Electrodes. *Sensor. Actuat. B: Chem.* **2012**, *169*, 182–187.
23. Lee, M.; Lee, J.; Kim, T. H.; Lee, H.; Lee, B. Y.; Park, J.; Jhon, Y. M.; Seong, M. J.; Hong, S. 100 nm Scale Low-Noise Sensors Based on Aligned Carbon Nanotube Networks: Overcoming the Fundamental Limitation of Network-Based Sensors. *Nanotechnology* **2010**, *21*, 055504.
24. Lee, M.; Noah, M.; Park, J.; Seong, M. J.; Kwon, Y. K.; Hong, S. "Textured" Network Devices: Overcoming Fundamental Limitations of Nanotube/Nanowire Network-Based Devices. *Small* **2009**, *5*, 1642–1648.
25. Peitz, I.; Fromherz, P. Electrical Interfacing of Neurotransmitter Receptor and Field Effect Transistor. *Eur. Phys. J. E* **2009**, *30*, 223–231.
26. Park, J.; Lim, J. H.; Jin, H. J.; Namgung, S.; Lee, S. H.; Park, T. H.; Hong, S. A Bioelectronic Sensor Based on Canine Olfactory Nanovesicle-Carbon Nanotube Hybrid Structures for the Fast Assessment of Food Quality. *Analyst* **2012**, *137*, 3249–3254.
27. Codignlona, A.; Tarroni, P.; Clementi, F.; Pollo, A.; Lovallo, M.; Carbone, E.; Sher, E. Calcium Channel Subtypes Controlling Serotonin Release Human Small Cell Lung Carcinoma Cell Lines. *J. Biol. Chem.* **1993**, *268*, 26240–26247.
28. Dobrydneva, Y.; Williams, R. L.; Morris, G. Z.; Blackmore, P. F. Dietary Phytoestrogens and Their Synthetic Structural Analogues as Calcium Channel Blockers in Human Platelets. *J. Cardiovasc. Pharmacol.* **1999**, *40*, 399–410.
29. Lee, B. Y.; Sung, M. G.; Lee, J.; Baik, K. Y.; Kwon, Y. K.; Lee, M. S.; Hong, S. Universal Parameters for Carbon Nanotube Network-Based Sensors: Can Nanotube Sensors Be Reproducible? *ACS Nano* **2011**, *5*, 4373–4379.